arXiv:1911.02935v1 [physics.atom-ph] 6 Nov 2019

Universal methods for suppressing the light shift in atomic clocks based on continuous-wave spectroscopy

V. I. Yudin,[1,2,3,4,*] M. Yu. Basalaev,[1,2,3] A. V. Taichenachev,[1,2] J. W. Pollock,[4,5]
Z. L. Newman,[4] M. Shuker,[4] A. Hansen,[4] M. T. Hummon,[4] E. A. Donley,[4] and J. Kitching[4]

[1] *Novosibirsk State University, ul. Pirogova 2, Novosibirsk, 630090, Russia*
[2] *Institute of Laser Physics SB RAS, pr. Akademika Lavrent'eva 13/3, Novosibirsk, 630090, Russia*
[3] *Novosibirsk State Technical University, pr. Karla Marksa 20, Novosibirsk, 630073, Russia*
[4] *National Institute of Standards and Technology, Boulder, Colorado 80305, USA*
[5] *University of Colorado, Boulder, Colorado 80309-0440, USA*

We develop previously unexplored methods for suppressing the light shift and its fluctuations in atomic clocks based on continuous-wave (CW) spectroscopy. These methods can be used for optical clocks on one- and two-photon transitions, as well as for rf clocks based on resonances of coherent population trapping and optical pumping clocks. These methods can be considered as CW analogs of recently-developed methods for Ramsey spectroscopy: a combined error signal in Ramsey spectroscopy [V. I. Yudin, *et al.*, New. J. Phys. **20**, 123016 (2018)] and generalized auto-balanced Ramsey spectroscopy [V. I. Yudin, *et al.*, Phys. Rev. Appl. **9**, 054034 (2018)], and which have already demonstrated their high efficiency in experiments. The proposed universal CW methods can be widely used both for high-precision scientific instruments and for commercial clocks of various types and purposes (including chip-scale atomic clocks), which have a huge sales market.

PACS numbers: 32.70.Jz, 06.30.Ft, 32.60.+i, 42.62.Fi

I. INTRODUCTION

Atomic clocks are currently one of the most sought-after quantum devices whose operation is based on quantum physics laws. These devices have a large scope both in fundamental physics (testing various fundamental theories in micro- and macro-physics) and in the field of practical applications (global position systems, ground and space navigation, telecommunications, geodesy, etc.). The current state of the art, problems, and some prospects for the further development of atomic clocks of various types and purposes are well-presented in reviews [1–4].

The most important metrological characteristics of an atomic clock are long-term stability and accuracy. In this case, one of the main factors limiting these characteristics is the light ac-Stark shift of atomic levels under the action of laser fields. Therefore, during the evolution of atomic frequency standards, special attention was paid and is being paid to the study of the light shift, as well as to the development of methods for its suppression. Particular successes in this direction have been achieved over the past decade for atomic clocks based on Ramsey spectroscopy. This process was begun in Ref. [5], where the method of the so-called hyper Ramsey spectroscopy was developed, which made it possible to reduce the light shift and its fluctuations for a reference atomic resonance by several orders of magnitude [6, 7]. Further development of the hyper-Ramsey approach has used new phase variants to build an error signal [8–14]. This allows for significant improvement in the efficiency of suppression of the light shift in atomic clocks.

Auto-balanced Ramsey spectroscopy (ABR) is another effective approach that was first experimentally demonstrated in a $^{171}Yb^{+}$ ion clock [15]. This approach was rigorously substantiated and generalized in Ref. [16], and also realized in atomic clocks based on coherent population trapping (CPT) [17, 18]. For ABR, in addition to the stabilization of the clock frequency, a second loop controls a variable second (concomitant) parameter, which is an adjustable property of the first and/or second Ramsey pulses. An alternative method named combined error signal (CES) spectroscopy has been recently proposed to form the error signal for the stabilization of Ramsey-based atomic clocks [19, 20]. In contrast to the ABR protocol, the Ramsey-CES method uses a single combined error signal, constructed by subtracting the error signals obtained from the two Ramsey sub-sequences with an appropriate normalization factor (calibration coefficient). This one-loop method offers light-shift mitigation and reduces the complexity of implementing the two-loop control system required for ABR-like protocols.

However, despite these significant advances in Ramsey spectroscopy, these successes had no significant effect on the development and improvement of commercial atomic clocks, which are in great demand and have different practical applications. This is because commercial clocks use, as a rule, continuous wave (CW) spectroscopy, while Ramsey spectroscopy is used very rarely. The main reason is that from the viewpoint of industrial production, the reliability and relative simplicity of devices come to the forefront, which makes CW spectroscopy in atomic vapor cells preferred. Moreover, in a number of important cases Ramsey spectroscopy does not make sense from a practical viewpoint at all. For example, such a situation holds true for modern opti-

*Electronic address: viyudin@mail.ru

cal clocks using vapor cells with alkali atoms as for one-photon sub-Doppler spectroscopy with counterpropagating waves at the S→P transition (e.g., see Ref. [21]), and also for two-photon spectroscopy at the S→D transition (eg, see Refs. [22–25]). Here, the practical inapplicability of the Ramsey protocol is connected to the short lifetime of the upper excited level (P or D). The same can be said about the atomic clock utilizing Doppler-free spectroscopy of molecular iodine in Ref. [26].

While CW spectroscopy has broader utility, universal methods to mitigate the light shift as with the ABR-like and CES-like protocols had not been developed. To date, several approaches to the problem of the light shift in CW spectroscopy are known for various types of clocks. The first efforts in this direction were made for rf CPT clocks, for which the light shift can be suppressed by a suitable choice of the rf modulation index of the laser field [27, 28]. However, that modulation index value is not optimal for the signal-to-noise ratio. For another type of rf clock based on optical pumping, a method of suppressing the light shift by the appropriate choice of the laser frequency $\omega_{\rm OP}$, which is used for optical pumping, was proposed in Ref. [29]. Recently, a method has been proposed that can suppress the light shift for two-photon spectroscopy at the transition $(5s\,^2S_{1/2}) \to (5d\,^2D_{5/2})$ in ^{87}Rb due to the use of two interrogating laser fields at different frequencies [30]. Therefore, the development of new effective and universal methods of suppressing the light shift for CW spectroscopy of clock transitions is currently a very relevant research topic.

In this paper, we develop two different methods for suppressing the light shift and its fluctuations in an atomic clock based on CW spectroscopy. Both methods use sequential alternating operations with two different laser powers P_1 and P_2. The first method operates with a single combined error signal (CW-CES), constructed by subtracting the error signals obtained from the two sub-sequences (P_1 and P_2) with an appropriate normalization factor (calibration coefficient) dependent on the ratio P_1/P_2. The second method uses a two-loop approach to feed back on and stabilize the clock frequency ω as well as a second (concomitant) parameter ξ, which determines the value of the artificial anti-shift of the clock transition, i.e., in this method we introduce an active auto-compensation of the shift (ACS). The operation of CW-ACS consists of the correlated stabilization of both variable parameters ω and ξ, which leads to the light shift cancelation for the clock frequency ω. Another variant of CW-ACS using low frequency harmonic power modulation is also proposed. Both the CW-CES and the CW-ACS methods are universal and can be applied in optical clocks using one-photon and two-photon spectroscopy, as well as in rf clocks based on CPT resonances and optical pumping clocks.

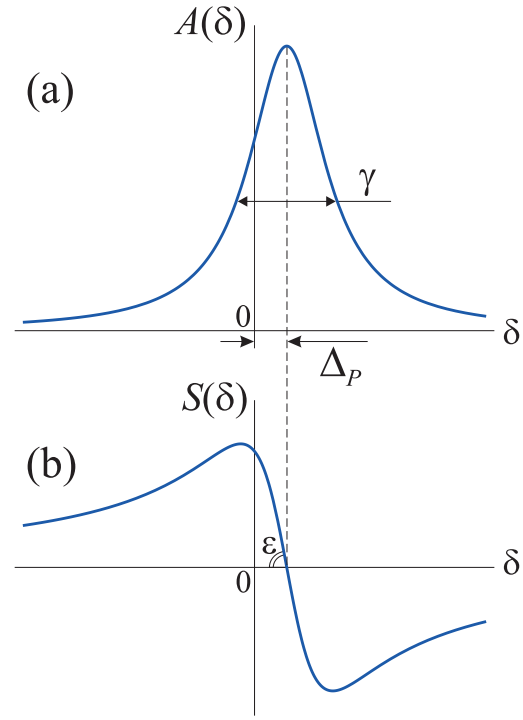

FIG. 1: (a) - the resonant lineshape of the spectroscopic signal $A(\delta)$ at the clock transition; (b) - the corresponding error signal $S(\delta)$.

II. GENERAL DESCRIPTION OF THE LIGHT SHIFT IN ATOMIC CLOCKS

Let us consider an atomic clock (both optical and rf ranges) in which the frequency of the local oscillator ω is stabilized by a reference atomic transition with an unperturbed frequency ω_0. For this purpose, a resonant spectroscopic signal with a characteristic linewidth γ [see Fig. 1(a)] is used, on the basis of which the dispersion-like error signal $S(\delta)$ is generated in some known way (e.g., by the use of harmonic frequency modulation or frequency jumps) as a function of the detuning $\delta = \omega - \omega_0$ [see Fig. 1(b)]. The standard operation of an atomic clock is to use a feedback loop to stabilize the frequency ω at the zero of the error signal:

$$S(\delta) = 0\,, \tag{1}$$

which, in the ideal case, corresponds to $\delta = 0$, i.e. $\omega = \omega_0$.

However, under the influence of a laser field, the resonant atomic transition experiences a light shift Δ_P [see Fig. 1(a)], which also manifests in the error signal [see Fig. 1(b)]. In this case, the frequency stabilization can be mathematically represented as

$$S(\delta - \Delta_P) = 0\,, \tag{2}$$

which leads to the following result

$$\delta = \Delta_P \;\Rightarrow\; \omega = \omega_0 + \Delta_P\,, \tag{3}$$

describing the light shift in an atomic clock. In this case, the main source of $\Delta_P \neq 0$ is the ac-Stark shift, which negatively affects not only the accuracy of atomic clocks, but also their long-term stability due to temporal variations in the value of $\Delta_P(t)$ caused by the power fluctuations of the laser field. Moreover, for rf clocks based on coherent population trapping, additional variations of $\Delta_P(t)$ can also occur from fluctuations in the modulation index of the laser field at the operating rf frequency ω. In the case of rf clocks based on optical pumping, additional variations of $\Delta_P(t)$ can be caused by fluctuations of the frequency $\omega_{\rm OP}$ of the laser which realizes optical pumping.

Below we consider two previously unknown methods for suppressing the ac-Stark shift and its variations in atomic clocks based on CW spectroscopy.

III. CW COMBINED ERROR SIGNAL

In this section, we describe the CW method of the combined error signal (CW-CES).

We will assume that the atomic clock operates at two different values of the probe laser field power, P_1 and P_2. For definiteness, we always assume $P_2 > P_1$. Moreover, we suppose that the following conditions are fulfilled:

1. The linearity of the light shift in power:

$$\Delta_P = cP\,, \tag{4}$$

where c is the empirical coefficient of proportionality.

2. Pure power-law dependence of the amplitude of the resonant signal and the slope of the error signal in the line center [see Fig. 1(b)]:

$$\tan\varepsilon = bP^{\alpha}\,, \tag{5}$$

where b and α can be arbitrary.

3. The light shift is much smaller than the linewidth:

$$\Delta_P \ll \gamma\,. \tag{6}$$

Let us consider now the error signals $S_{P_1}(\delta)$ and $S_{P_2}(\delta)$ for two values P_1 and P_2. Because of condition (6), near the zero of the error signals, the linear approximation can be used with good accuracy, as shown in Fig. 2(a). Using well-known trigonometric formulas, we find the ratio of the segments $0A_2$ and $0A_1$ in Fig. 2(a):

$$\frac{0A_2}{0A_1} = \frac{\Delta_{P_2}\tan\varepsilon_2}{\Delta_{P_1}\tan\varepsilon_1} = \left(\frac{P_2}{P_1}\right)^{\alpha+1}, \tag{7}$$

where we used expressions (4) and (5). If we multiply the error signal $S_{P_2}(\delta)$ by the calibration coefficient $\beta_{\rm cal}$, which is inverse to the ratio (7):

$$\beta_{\rm cal} = \left(\frac{P_1}{P_2}\right)^{\alpha+1}, \tag{8}$$

then the dependence $\beta_{\rm cal}S_{P_2}(\delta)$ will cross another error signal $S_{P_1}(\delta)$ at the point A_1 [as shown in Fig. 2(b)],

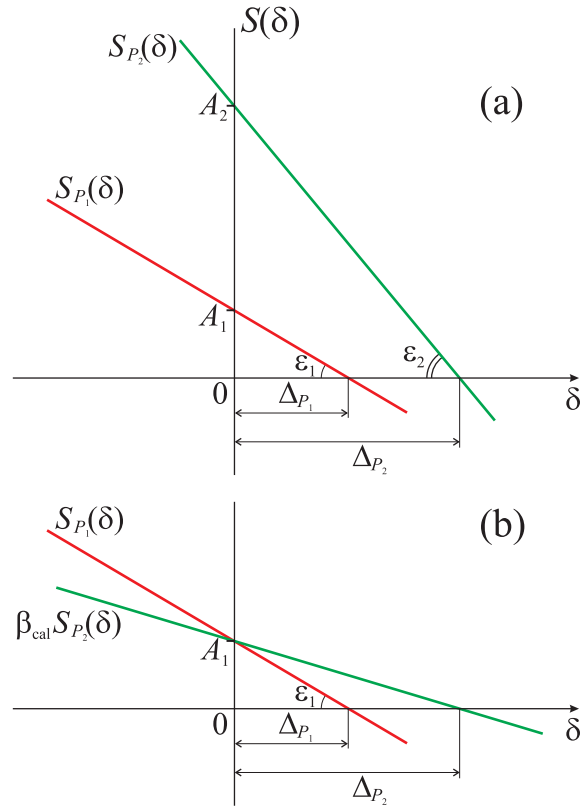

FIG. 2: (a) - linear central sections of the error signals $S_{P_1}(\delta)$ (red line) and $S_{P_2}(\delta)$ (green line) taking into account light shifts Δ_{P_1} and Δ_{P_2}; (b) - transformation of the upper figure (a) when instead of the dependence $S_{P_2}(\delta)$, the product $\beta_{\rm cal}S_{P_2}(\delta)$ is presented (green line), in which the calibration coefficient $\beta_{\rm cal}$ [see Eq. (8)] is used.

which is located on the vertical axis corresponding to the unshifted frequency, $\delta = 0$. As a result, if we construct a combined error signal (CW-CES) as

$$S_{\rm CES}(\delta) = S_{P_1}(\delta) - \beta_{\rm cal}S_{P_2}(\delta)\,, \tag{9}$$

then the dependence $S_{\rm CES}(\delta)$ will cross the horizontal axis at the point $\delta = 0$, as shown in Fig. 3. Thus, if we use CW-CES (9) to stabilize the frequency ω, as a result we get:

$$S_{\rm CES}(\delta) = 0 \;\Rightarrow\; \delta = 0 \;\Rightarrow\; \omega = \omega_0\,, \tag{10}$$

which means that the atomic clock light shift and its variations are suppressed. In addition, to maximize $S_{\rm CES}(\delta)$, the condition $P_2 \gg P_1$ should hold.

A general scheme of the experimental implementation of CW-CES is presented in Fig. 4. The power modulator (PM) creates an alternating sequence of two different powers P_1 and P_2 of the laser. Note that, for example, an acousto-optical modulator or a liquid crystal followed by a polarizer can be used as the PM. Next, before entering the atomic cell, a beam-splitter is installed, which splits the laser beam into two. One of them passes through the atomic cell and forms a spectroscopic signal and error

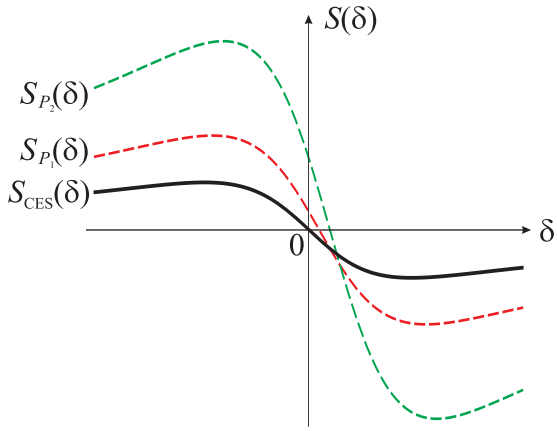

FIG. 3: Illustration showing the absence of a light shift for the combined error signal $S_{\rm CES}(\delta)$ (black solid line), while the common error signals $S_{P_1}(\delta)$ (red dashed line) and S_{P_2} (green dashed line) experience light shifts.

signals $S_{P_1}(\delta)$ and $S_{P_2}(\delta)$ using the first photodetector PD_1. In the case of one-photon spectroscopy, this can be a transmission signal, while in the case of two-photon spectroscopy, this can be a fluorescence signal. The second beam is incident on photodetector PD_2 and is used to calculate the ratio P_1/P_2, i.e., to determine the calibration coefficient $\beta_{\rm cal}$ [see Eq. (8)]. The digital block "N-box" based on data from the photodetectors PD_1 and PD_2 generates the combined error signal $S_{\rm CES}(\delta)$ [see Eq. (9)], which is then used to stabilize the frequency ω of the local oscillator (LO) by the condition $S_{\rm CES}(\delta) = 0$.

CW-CES is a quite universal method suitable for various types of spectroscopy. For example, for one-photon spectroscopy in counterpropagating waves and in the weak saturation regime of the clock transition we have $\alpha = 1$. In this case, the calibration coefficient is:

$$\beta_{\rm cal}^{\rm (1\text{-}ph)} = \left(\frac{P_1}{P_2}\right)^2 . \tag{11}$$

In the case of a fluorescence signal for two-photon spectrocopy, $\alpha = 2$, i.e., the calibration coefficient is:

$$\beta_{\rm cal}^{\rm (2\text{-}ph)} = \left(\frac{P_1}{P_2}\right)^3 . \tag{12}$$

CW-CES can also be used in CPT clocks as well as for optical pumping clocks. In general, the success of the CW-CES method is directly related to how accurately the basic conditions (4)-(6) are fulfilled in experiments.

In addition, in some cases, to obtain information about the laser power P, we can also use the first photodetector PD_1. In this case, the presence of a second photodetector PD_2 is optional, which provides some technical simplification. Note also that the CW-CES method presented above can ideologically be considered the CW analog of the Ramsey-CES method developed in Ref. [19].

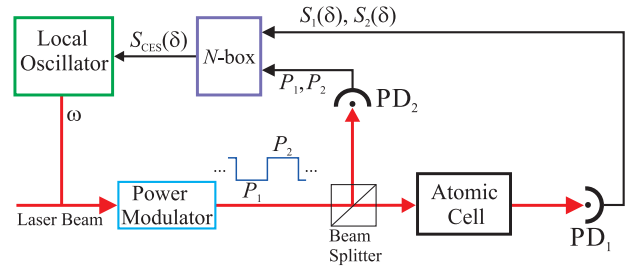

FIG. 4: The general scheme of the experimental implementation of the CW-CES method.

IV. AUTO-COMPENSATION OF THE LIGHT SHIFT (CW-ACS)

In this section, we develop a method to auto-compensate the light shift (ACS) in CW spectroscopy (CW-ACS). Unlike the CW-CES method developed in the previous section, CW-ACS only requires the linearity of the light shift (4), while the other two conditions (5) and (6) do not matter. In CW-ACS, we assume the use of an additional electronic block (frequency shifter), which for any laser power P allows us to shift the frequency of the local oscillator ω by the value ξP, where ξ is a well-controlled and variable parameter. This shift ξP plays the role of an artificial anti-shift, which allows us to completely compensate for the actual light shift $\Delta_P = cP$ and its fluctuations. Indeed, taking into account the actual shift Δ_P and the artificial anti-shift ξP, the result of the frequency stabilization with the use of the error signal can be represented as a solution of the equation

$$S_P(\delta, \xi) = S_P(\delta + \xi P - cP) = 0 \tag{13}$$

for an unknown δ. Then, obviously, for $\xi = c$ we get $\delta = 0$, i.e. $\omega = \omega_0$.

Below we present the implementation of the CW-ACS method in two different modifications: for stepwise and harmonic modulations of the laser power.

a) CW-ACS for stepwise modulation of power

We will assume that the atomic clock operates at two different values of the probe laser field power P_1 and P_2. The CW-ACS method consists of the following repeating cycles. For interrogation with the laser power P_1, the parameter ξ is fixed, and we stabilize the variable detuning δ (i.e., LO frequency ω) at the zero point of the error signal: $S_{P_1}(\delta, \xi_{fixed}) = 0$. After this procedure, we switch to interrogation with power P_2, where we fix the previously-obtained detuning δ and stabilize the variable parameter ξ at the zero point of the second error signal: $S_{P_2}(\delta_{fixed}, \xi) = 0$. If we continue these cycles, then the final result consists of the stabilization of both parameters, $\delta = \bar{\delta}_{\rm clock}$ and $\xi = \bar{\xi}$, which corresponds to the

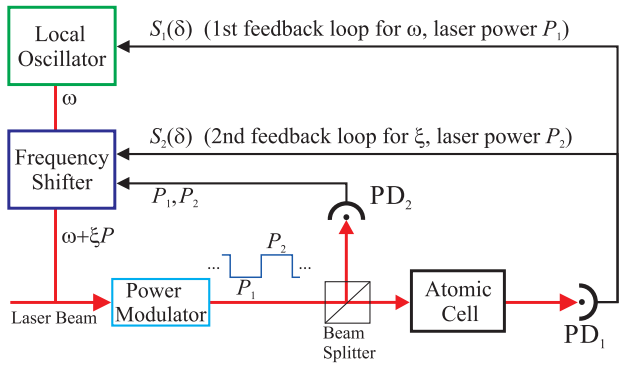

FIG. 5: The general scheme of the experimental implementation of the CW-ACS method for stepwise modulation of power.

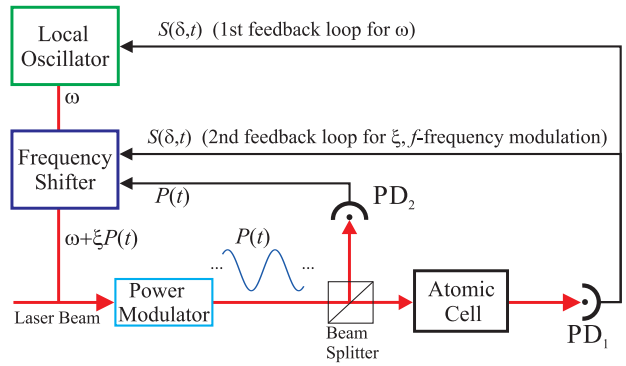

FIG. 6: The general scheme of the experimental implementation of the CW-ACS method for low-frequency harmonic modulation of laser power (17).

solution of a system of two equations:

$$S_{P_1}(\delta,\xi) = S_{P_1}(\delta + \xi P_1 - cP_1) = 0$$
$$S_{P_2}(\delta,\xi) = S_{P_2}(\delta + \xi P_2 - cP_2) = 0\,, \qquad (14)$$

for two unknowns δ and ξ. The value $\bar{\delta}_{\rm clock}$ describes the frequency shift in an atomic clock. The Eqs. (14) are equivalent to the system given by

$$\delta + (\xi - c)P_1 = 0\,, \quad \delta + (\xi - c)P_2 = 0\,, \qquad (15)$$

which obviously has the solution

$$\delta = 0\,, \quad \xi = c\,. \qquad (16)$$

Thus, we have shown that the CW-ACS method always leads to zero shift of the stabilized frequency ω in an atomic clock, $\bar{\delta}_{\rm clock} = 0$.

Fig. 5 shows a schematic diagram of the implementation of the CW-ACS method, which has two feedback loops to stabilize δ and ξ. In this case, the first photodetector PD$_1$ is used to generate the error signals $S_{P_1}(\delta,\xi)$ and $S_{P_2}(\delta,\xi)$, while for the implementation of the artificial anti-shift ξP the readings of the second photodetector PD$_2$ are used. CW-ACS is a universal method for clocks based on various types of atomic spectroscopy. It can be either an optical clock using one-photon and two-photon spectroscopy, or an rf clock based on CPT resonances and optical pumping clocks.

Note that the permanent use of two feedback loops (for P_1 and P_2) will lead to some decrease of the short-term stability, because it increases the length of each cycle of stabilization. Therefore, from our viewpoint, the more favorable scenario is the following. In the initial period of frequency stabilization, we use the two-loop CW-ACS method. It allows us to determine the value of the concomitant parameter $\bar{\xi}$ with satisfactory accuracy. Then the procedure of long-term frequency stabilization can be done by only one feedback loop for the error signal $S_{P_1}(\delta,\bar{\xi})$ using the previously-determined parameter $\bar{\xi}$. Moreover, we can regularly (but rarely) use the two-loop CW-ACS again. First, it allows us to do a regular adjustment of the parameter $\bar{\xi}$ (to eliminate, for example, an influence of possible slow variations and degradation of the electronic characteristics of the second photodetector PD$_2$). Second, such intermittent application of CW-ACS will not lead to significant slowing-down of long-term frequency stabilization. In addition, Fig. 5 shows a scheme in which we assumed for definiteness, $P_1 < P_2$. However, for real experiments, the ratio between the powers P_1 and P_2 should be chosen from the optimization of the frequency stabilization procedure.

We stress that the success of the CW-ACS method is directly related to how accurately the linearity condition (4) is met. In this context, it seems very relevant to continue a detailed study of light shifts for various atomic clocks in order to determine the most suitable operating modes in which the linearity condition (4) is best fulfilled.

We also note that the CW-ACS method can ideologically be considered as a CW analog of one of the variants of generalized auto-balance Ramsey spectroscopy Ref. [16, 18], in which an additional frequency shift was used as the concomitant parameter.

b) CW-ACS for low frequency harmonic modulation of power

Fig. 6 shows a schematic diagram of the implementation of another version of CW-ACS using low-frequency harmonic modulation of the laser power:

$$P(t) = P_0\,[1 + M\sin(ft)]\,, \qquad (17)$$

where $M < 1$. In this case, both the actual shift $\Delta_P(t) = cP(t)$ and the artificial anti-shift $\xi P(t)$ become time-dependent according to a harmonic law with a frequency f. Note that the power modulation frequency f is much lower than the frequency of the frequency deviation used to generate the error signal $S(\delta)$, as was in Ref. [28] for CPT clock.

The operation of the scheme in Fig. 6 is the following. The effect of power modulation (17) is monitored as modulation on the error signal $S(\delta,t)$ at the frequency f. This

low-frequency modulation is observed on the error signal because a change in the total optical power produces a corresponding change in the atomic resonance frequency due to both the actual light shift $\Delta_P(t) = cP(t)$ and the artificial anti-shift $\xi P(t)$:

$$cP(t) - \xi P(t) = (c - \xi)P(t)\,. \tag{18}$$

Then, the condition $\xi = c$ at which the power shift contribution (18) becomes zero occurs when the f-frequency modulation on the error signal vanishes.

V. CONCLUSION

We have developed two different methods for suppressing the light shift and its fluctuations in atomic clocks based on CW spectroscopy. The first CW-CES method uses only one feedback loop to stabilize the LO frequency. Another CW-ACS method has two loops: in addition to the feedback loop for stabilizing the LO frequency ω, there is a second feedback loop for stabilizing the concomitant parameter ξ. These methods are universal and can be applied in optical clocks using one-photon and two-photon spectroscopy, as well as in rf clocks based on CPT resonances and optical pumping clocks. We believe that the implementation of the CW-CES and CW-ACS techniques can lead to significant improvement of the accuracy and long-term stability for high-precision atomic clocks as well as for commercial atomic clocks of wide application (including chip-scale atomic clocks).

Acknowledgments

We thank Sihong Gu and Leo Hollberg for useful discussions. This work was supported by the Russian Scientific Foundation (No. 16-12-10147). A. V. Taichenachev was supported by the Russian Foundation for Basic Research (No. 18-02-00822). This work is also funded by NIST, an agency of the U.S. government, and is not subject to copyright.

[1] V. Shah and J. Kitching, Adv. At. Mol. Opt. Phys. **59**, 21 (2010).
[2] N. Poli, C. W. Oates, P. Gill, and G. M. Tino, Rivista Del Nuovo Cimento **36**, 555 (2013).
[3] A. D. Ludlow, M. M. Boyd, J. Ye, E. Peik, and P. O. Schmidt, Optical atomic clocks, Rev. Mod. Phys. **87**, 637 (2015).
[4] B. L. Schmittberger and D. R. Scherer, MITRE Technical Report, MTR190551 (2019).
[5] V. I. Yudin, A. V. Taichenachev, C. W. Oates, Z. W. Barber, N. D. Lemke, A. D. Ludlow, U. Sterr, Ch. Lisdat, and F. Riehle, Hyper-Ramsey spectroscopy of optical clock transitions, Phys. Rev. A **82**, 011804(R) (2010).
[6] N. Huntemann, B. Lipphardt, M. Okhapkin, Chr. Tamm, E. Peik, A. V. Taichenachev, and V. I. Yudin, Generalized Ramsey excitation scheme with suppressed light shift, Phys. Rev. Lett. **109**, 213002 (2012).
[7] N. Huntemann, C. Sanner, B. Lipphardt, Chr. Tamm, and E. Peik, Single-ion atomic clock with 3×10^{-18} systematic uncertainty, Phys. Rev. Lett. **116**, 063001 (2016).
[8] R. Hobson, W. Bowden, S. A. King, P. E. G. Baird, I. R. Hill, P. Gill, Modified hyper-Ramsey methods for the elimination of probe shifts in optical clocks, Phys. Rev. A **93**, 010501(R) (2016).
[9] T. Zanon-Willette, S. Almonacil, E. de Clercq, A. D. Ludlow, and E. Arimondo, Quantum engineering of atomic phase shifts in optical clocks, Phys. Rev. A **90**, 053427 (2014).
[10] T. Zanon-Willette, E. de Clercq, and E. Arimondo, Probe light-shift elimination in generalized hyper-Ramsey quantum clocks, Phys. Rev. A **93**, 042506 (2016).
[11] V. I. Yudin, A. V. Taichenachev, M. Yu. Basalaev, and T. Zanon-Willette, Synthetic frequency protocol for Ramsey spectroscopy of clock transitions, Phys. Rev. A **94**, 052505 (2016).
[12] T. Zanon-Willette, V. I. Yudin, and A. V. Taichenachev, Generalized hyper-Ramsey resonance with separated oscillating fields, Phys. Rev. A. **92**, 023416 (2015).
[13] T. Zanon-Willette, R. Lefevre, A. V. Taichenachev, and V. I. Yudin, Universal interrogation protocol with zero probe-field-induced frequency shift for quantum clocks and high-accuracy spectroscopy, Phys. Rev. A **96**, 023408 (2017).
[14] T. Zanon-Willette, R. Lefevre, R. Metzdorff, N. Sillitoe, S. Almonacil, M. Minissale, E. de Clercq, A. V. Taichenachev, V. I. Yudin, and E. Arimondo, Rep. Prog. Phys. **81**, 094401 (2018).
[15] Ch. Sanner, N. Huntemann, R. Lange, Ch. Tamm, and E. Peik, Autobalanced Ramsey spectroscopy, Phys. Rev. Lett. **120**, 053602 (2018).
[16] V. I. Yudin, A. V. Taichenachev, M. Y. Basalaev, T. Zanon-Willette, J. W. Pollock, M. Shuker, E. A. Donley, and J. Kitching, Phys. Rev. Applied **9**, 054034 (2018).
[17] M. Abdel Hafiz, G. Coget, P. Yun, S. Guérandel, E. de Clercq, and R. Boudot, J. Appl. Phys. **121**, 104903 (2017).
[18] M. Shuker, J. W. Pollock, R. Boudot, V. I. Yudin, A. V. Taichenachev, J. Kitching, and E. A. Donley, Phys. Rev. Lett. **122**, 113601 (2019).
[19] V. I. Yudin, A. V. Taichenache, M. Yu. Basalaev, T. Zanon-Willette, T. E. Mehlstäubler, R. Boudot, J. W. Pollock, M. Shuker, E. A. Donley, and J. Kitching, New J. Phys. **20**, 123016 (2018).
[20] M. Shuker, J. W. Pollock, R. Boudot, V. I. Yudin, A. V. Taichenachev, J. Kitching, and E. A. Donley, Appl. Phys. Lett. **114**, 141106 (2019).
[21] M. Abdel Hafiz, G. Coget, E. De Clercq, and R. Boudot, Opt. Lett. **41**, 2982 (2016).
[22] C. Perrella, P. S. Light, J. D. Anstie, T. M. Stace, F. Ben-

abid, and A. N. Luiten, Phys. Rev. A **87**, 013818 (2013).
[23] C. Perrella, P. S. Light, J. D. Anstie, F. N. Baynes, F. Benabid, and A. N. Luiten, Opt. Lett. **38**, 2122 (2013).
[24] K. W. Martin, G. Phelps, N. D. Lemke, M. S. Bigelow, B. Stuhl, M. Wojcik, M. Holt, I. Coddington, M. W. Bishop, and J. H. Burke, Phys. Rev. Applied, **9**, 014019, (2018).
[25] K. W. Martin, B. Stuhl, J. Eugenio, M. S. Safronova, G. Phelps, J. H. Burke, and N. D. Lemke, Phys. Rev. A **100**, 023417 (2019).
[26] T. Schuldt, K. Dringshoff, E. Kovalchuk, J. Pahl, M. Gohlke, D. Weise, U. Johann, A. Peters, and C. Braxmaier, Proceedings Volume 10563, International Conference on Space Optics ICSO 2014; 105632S (2017).
[27] M. Zhu and L. S. Cutler, in *Proceedings of 32th Annual Precise Time and Time Interval Systems and Applications Meeting (Institute of Navigation, Inc., Reston, Virginia, 2000)*, pp. 311324.
[28] V. Shah, V. Gerginov, P. D. D. Schwindt, S. Knappe, L. Hollberg, and J. Kitching, Appl. Phys. Lett. **89**, 151124 (2006).
[29] B. H. McGuyera, Y.-Y. Jau, and W. Happer, Appl. Phys. Lett. **94**, 251110 (2009);
[30] V. Gerginov and K. Beloy, Phys. Rev. Applied **10**, 014031 (2018).